Journal of Materials Chemistry C

PAPER

View Article Online
View Journal | View Issue

Cite this: J. Mater. Chem. C, 2019, 7, 10972

Lanthanide grafted phenanthroline-polymer for physiological temperature range sensing†

Flore Vanden Bussche, ‡[ab] Anna M. Kaczmarek, ‡[b] Johannes Schmidt,[c] Christian V. Stevens *[a] and Pascal Van Der Voort *[b]

Received 2nd May 2019,
Accepted 16th August 2019

DOI: 10.1039/c9tc02328c

rsc.li/materials-c

Accurate measurement of the temperature is crucial as it determines the dynamics of almost any system. Conventional contact thermometers are not well suited for small scale measurements. Temperature dependent luminescent materials, *i.e.* materials that emit light of different color at different temperature, are therefore of particular interest in the development of noncontact thermometers. Luminescent materials consisting of lanthanide ions feature high thermal sensitivity, high photostability and high quantum yields. These ions possess very interesting light emitting properties. By anchoring them onto different backbone materials, their light absorption is increased. The search for a backbone that allows the sensor to be active in a defined temperature range, with a high detection sensitivity is ongoing. This work reports the first insoluble phenanthroline-polymer (phen-polymer) backbone on which europium (Eu^{3+}) and terbium (Tb^{3+}) trifluoroacetylacetone (tfac) complexes are easily grafted in a 1:1 metal ratio in order to create a noncontact temperature sensor. Two clear, discriminable emission peaks were observed during the photoluminescence study at room temperature, demonstrating that this material can be used as a ratiometric thermometer. The characteristic emission peak correlated to Eu^{3+} transition is slightly stronger than the emission peak of Tb^{3+} transition, resulting in a yellow emission color. The maximum value of the relative temperature sensitivity was calculated to be 2.3404% K^{-1} (340 K), which indicated good thermometric behavior. The emission color of the designed phen-polymer@Eu,Tb_tfac changed from light green (260 K) to orange-red (460 K). The thermometer can therefore be used as a ratiometric noncontact temperature sensor in the broad physiological temperature range.

Introduction

Temperature is a crucial physical variable that affects viability and dynamics of nearly all natural and engineered systems.[1] An accurate measurement of temperature is therefore essential in countless technological and industrial developments and in scientific research. Temperature measurements are performed with contact or noncontact temperature sensors. Contact thermometers are not appropriate for small scale samples due to the direct contact and disruption of the sample temperature.[2] Noncontact thermometers are therefore highly desirable in areas such as microelectronics, microfluids and nanomedicine. Luminescent materials are increasingly investigated as noncontact temperature sensors, because their luminescence can be dependent on the temperature.[2] These materials often consist of trivalent lanthanide ions (Ln^{3+}) that are grafted or doped onto inorganic or organic–inorganic hybrid compounds.[3,4] Lanthanide ions possess very interesting light emitting properties. Their luminescence is a result of transitions within their partially filled 4f shells.[5] This leads to narrow emission peaks from the ultraviolet-visible to near-infrared region. Moreover, Ln^{3+} ions have significantly long decay times as well as high quantum yields. The 4f–4f transitions are however parity-forbidden, resulting in low molar absorption coefficients. To conquer the low molar absorption coefficients and thus increase the light absorption, various inorganic materials and hybrid materials have been developed. These materials are suitable for complexation of lanthanide ions and they can act as antenna, which means they enable exciting the Ln^{3+} ions through charge-transfer bands or organic ligands, thereby creating highly luminescent materials.[6,7] Among some of the most common hybrid materials are Metal Organic Frameworks (MOFs), coordination polymers and β-diketonate complexes. The luminescence of these materials when doped or grafted with Ln^{3+} has been extensively studied and reported in literature.[8–12] Organic polymers grafted with

[a] Synthesis, Bioresources and Bioorganic Chemistry Research Group (SynBioC), Department of Green Chemistry and Technology, Ghent University, Campus Coupure, Coupure Links 653, 9000 Ghent, Belgium. E-mail: Chris.stevens@ugent.be
[b] Center for Ordered Materials, Organometallics and Catalysis (COMOC), Department of Chemistry, Ghent University, Krijgslaan 281 S3, 9000 Ghent, Belgium. E-mail: Pascal.vandervoort@ugent.be
[c] Department of Chemistry, Division of Functional Materials, Technische Universität Berlin, Hardenbergstraße 40, 10623, Berlin, Germany

† Electronic supplementary information (ESI) available. See DOI: 10.1039/c9tc02328c

‡ These authors made equivalent contributions.

lanthanide ions are much less explored up to date, yet present a very interesting class of materials.[13–15]

Lanthanide compounds can be ideally used as sensor as they cover virtually the whole electromagnetic spectrum ranging from UV (gadolinium, Gd^{3+}) to near-infrared (erbium, Er^{3+}).[11] A thermometer should preferably have two discriminable emission peaks in order to observe a clear luminescence and coherent temperature difference. The ratio of the two peak intensities creates a reliable ratiometric thermometer that is independent of (i) the excitation source (ii) the concentration and inhomogeneity of the luminescent centers in the material (iii) the detector. A universal thermometer does however not exist, as different applications require different properties. Several temperature regions can be identified: cryogenic (up to 100 K), medium (100–300 K), biological/physiological (298–323 K) and the high temperature region (400 K). So far a wide range of materials has been studied for their potential use as luminescence ratiometric thermometers and among them MOFs and inorganic phosphors have been reported most frequently.[9,16–18] Other less common materials such as polyoxometalates (POMs) or POM@MOFs, polymer films and hybrid materials have also recently been reported.[19–24] Soluble, organic polymers doped with europium or terbium have been investigated for their use as non-ratiometric temperature-sensitive paint.[15,28] It is without doubt interesting to study novel classes of materials for the development of ratiometric temperature sensors, as new, interesting properties may emerge. Therefore, in this work we have developed an insoluble organic polymer, containing phenanthroline half-open loops that are ideally suited for grafting lanthanide ions through coordination bonds of the nitrogen rich pockets with the metal center.[25] We have focused on the luminescence properties and temperature-dependent luminescence properties of the phenanthroline-polymer (phen-polymer) when grafted with europium (Eu^{3+}), terbium (Tb^{3+}) and Eu^{3+}/Tb^{3+} trifluoroacetylacetone (tfac) complexes. The trifluoroacetylacetone ligand has a dual role, it acts as a secondary ligand to protect the first coordination sphere of the lanthanides from quenching by H_2O molecules (detrimental to luminescent properties) and it works as a second antenna for the absorption of light. This thermometer shows good performance from 260–460 K. It could therefore find use as a temperature sensor in chemical reactors or for biomedical applications, although it should be mentioned here that biological tests would first be needed to determine if the material is nontoxic.[26,27,35]

Experimental section

Materials

All chemicals were purchased from Sigma Aldrich and TCI Europe. The solvents used in the preparation were reagent grade and were not purified further. All commercially available reagents were used as received.

Synthesis and characterization of the insoluble phen-polymer

The insoluble phenanthroline-polymer (phen-polymer) was obtained in a one-step synthesis procedure. The starting material 1,10-phenanthroline-2,9-dicarbaldehyde was synthesized according to an optimized literature procedure. The synthesis and characterization can be found in the ESI.† [29] In a 100 mL Erlenmeyer flask 0.1 mmol 1,10-phenanthroline-2,9-dicarbaldehyde and 0.1 mmol (1,1′-biphenyl)-3,3′,4,4′-tetramine hydrochloride were weighed off. The materials were dissolved in 12 mL dioxane and 8 mL mesitylene in an ultrasonic bath for 15 minutes. 1.2 mL of 6 M acetic acid was dropwise added under slow shaking of the mixture. The Erlenmeyer flask was capped and stored undisturbed for 48 h. The resulting orange precipitate was collected by filtration and washed with methanol and acetone. To fully remove unreacted monomer, the solid was further washed in a 500 mL flask by stirring in 300 mL dichloromethane under reflux for 24 h. The final product was dried overnight under vacuum at 70 °C, resulting in an orange powder obtained in 87% yield. The characterization of the insoluble polymer is done according to other reported insoluble polymers.[30] These characterization techniques include Fourier Transform Infrared Spectrophotometer (FTIR) spectroscopy, thermogravimetrical analysis (TGA), elemental analysis, X-ray photoelectron spectroscopy (XPS), powder X-ray diffraction (PXRD) analysis, Brunauer–Emmett–Teller (BET) surface area, transmission electron microscopy-energy-dispersive X-ray spectroscopy (TEM/EDX) and scanning electron microscopy (SEM). IR spectra with a S/N-ratio of 30 000 : 1 were obtained from samples in neat form with a Quest ATR (Attenuated Total Reflectance) accessory with diamond crystal puck using a Shimadzu IRAFFINITY-1S Fourier Transform Infrared Spectrophotometer (FTIR). TA Netzsch Model STA 449 F3 Jupiter system was used to perform thermogravimetrical analysis (TGA) under N_2 flow (100 mL min^{-1}). For CHNS elemental analysis, a Thermo Flash 2000 thermal analyser (Thermo Scientific) is used with V_2O_5 as catalyst and methionine as standard. X-ray photoelectron spectroscopy (XPS) measurement was performed using a Thermo Scientific K-Alpha X-ray Photoelectron Spectrometer. The sample was analyzed using a microfocused, monochromated Al Kα X-ray source (1486.68 eV; 400 μm spot size). The K-Alpha charge compensation system was employed during analysis to prevent any localized charge buildup. Powder X-ray powder diffraction (PXRD) pattern was collected on a Thermo Scientific ARL X'Tra diffractometer, operated at 40 kV, 30 mA using Cu Kα radiation (λ = 1.5406 Å). The specific Brunauer–Emmett–Teller (BET) surface area was measured on a Belsorp Mini apparatus at 77 K. Prior to analysis, the sample was dried at 100 °C under vacuum for 24 h. HAADF-STEM and the EDX mapping analysis was performed using JEOL JEM-2200FS High-Resolution STEM equipped with an EDX spectrometer with a spatial resolution of 0.13 nm, image lens spherical aberration corrector, electron energy loss spectrometer (filter) and an emission field gun (FEG) operating at 200 keV. Secondary electron images were taken on a JEOL JSM-7600F FEG SEM apparatus. Goldsputtering was used prior to analysis.

Synthesis and characterization of the lanthanide phen-polymer thermometer

The samples were prepared by weighting of 0.002 mmol of the sample and a 5 times molar excess of the pre-synthesized $Ln(tfac)_3{\cdot}2H_2O$ complexes and placing it in a Pyrex tube. 5 mL

of methanol was added and the tube was sealed and placed in the ultrasound bath for 10 minutes for the powder to disperse in the methanol. Next, the tube was placed on a heating block at 80 °C and the reaction was carried out for 24 h. Afterwards the powder was filtered and washed with a small amount of methanol and dried in an oven at 80 °C.

The luminescence of solid samples was studied. Solid powdered samples were put between quartz plates (Starna cuvettes for powdered samples, type 20/C/Q/0.2). Colloidal suspensions were measured in quartz cuvettes with a path length of 10 mm. Luminescence measurements were performed on an Edinburgh Instruments FLSP920 UV-vis-NIR spectrometer setup. A 450 W xenon lamp was used as the steady state excitation source. Luminescence decay times were recorded using a 60 W pulsed Xe lamp, operating at a frequency of 100 Hz. A Hamamatsu R928P photomultiplier tube was used to detect the emission signals in the near UV to visible range. All of the luminescence measurements were recorded at room temperature unless indicated otherwise. In order to compare the measurements, the same amounts of powders were used as well as the same settings for each measurement (same slit size, step, and dwell time). All emission spectra in the manuscript have been corrected for detector response. The luminescence decay curves of the samples were measured when excited into the maximum of the broad ligand band and monitored at the appropriate wavelength (strongest peak of the given lanthanide). All of the decay curves could be well fitted using either a single exponential function or biexponential function.

$$I = A\ \exp\left(-\frac{t}{\tau}\right)$$

$$I = A_1\ \exp\left(-\frac{t}{\tau_1}\right) + A_2\ \exp\left(-\frac{t}{\tau_2}\right)$$

where I represents the luminescence intensity of a transition and A, A_1 and A_2 are constants, t is time and τ, τ_1 and τ_2 are the luminescence lifetimes.

Absolute quantum yields (QY) were measured by using an integrated sphere with a BENFLEC coating provided by Edinburgh Instruments as follows:

$$\eta = \frac{\int L_{\text{emission}}}{\int E_{\text{blank}} - \int E_{\text{sample}}}$$

where L_{emission} is the integrated value of the emission spectrum, and E_{blank} and E_{sample} are the integrated values of the "excitation" band of the blank and the excitation band of the sample (since the sample absorbs part of the light, this value will be smaller than E_{blank}), respectively.

The temperature-measurements were performed using an ARS closed cycle cryostat at a temperature range between 260–460 K. For the conversion of intensity into temperature the thermometric parameter Δ was employed. Here, $\alpha = W_0/W_R$ is the ratio between the nonradiative (W_0 at T = 0 K) and radiative (W_R) rates, ΔE is the activation energy for the nonradiative channel, and Δ_0 is the thermometric parameter at T = 0 K.

$$\Delta = \frac{I_1}{I_2} = \frac{\Delta_0}{1 + \alpha\ \exp\left(-\frac{\Delta E}{k_B T}\right)}$$

The relative temperature sensitivity S_r was calculated using the following equation:

$$S_r = 100\% \times \left|\frac{1}{\Delta}\frac{\partial \Delta}{\partial T}\right|$$

S_r indicates the relative change of the thermometric parameter per degree of temperature change (% K^{-1}). Compared with S_a, S_r has the important advantage of being independent of the nature of the thermometer and allows direct and quantitative comparison of different materials.

Another important parameter when assessing the performance of a thermometer is the temperature uncertainty δT. It can be determined using the following equation:

$$\delta T = \frac{1}{S_r}\frac{\delta \Delta}{\Delta}$$

where $\frac{\delta \Delta}{\Delta}$ is the relative error in the determination of the thermometric parameter. The repeatability of the thermometer was calculated employing equation:

$$R = 1 - \frac{\max|\Delta c - \Delta i|}{\Delta c}$$

where Δc is the mean thermometric parameter and Δi is the value of each measurement of thermometric parameter.

Results and discussion

The temperature sensor was developed in three main steps. First, the insoluble phenanthroline-polymer was synthesized and characterized. Second, Eu^{3+}, Tb^{3+} and Eu^{3+}/Tb^{3+} trifluoroacetylacetone (tfac) complexes were grafted onto the material. In a last step, the luminescence and temperature-dependent luminescence properties of the novel material were investigated. A schematic overview of the synthetic route is given in Fig. 1. Phenanthroline moieties were implemented in the insoluble polymer to create ideal complexation spheres for lanthanide ions.[5] The polymer was prepared by a condensation reaction of 1,10-phenanthroline-2,9-dicarbaldehyde and (1,1′-biphenyl)-3,3′,4,4′-tetramine. This reaction created imidazole linkages between the phenanthroline building blocks. The insolubility of the polymer was confirmed by solubility tests in water and a variety of organic solvents (both polar and nonpolar), such as methanol, ethanol, tetrahydrofuran, dichloromethane, acetonitrile, dimethyl formamide, dimethyl sulfoxide, diethyl ether and chloroform. The insoluble character of the polymer is interesting as it simplifies its separation from solvent mixtures.

The polymer was investigated by FTIR, TGA, XPS, PXRD, BET surface area and elemental analysis. Further characterization results (SEM) can be found in the ESI,† (SI2). The FTIR spectrum (Fig. 2) reveals the formation of imidazole linkages, confirmed by a weak, single broad peak for N–H stretching of

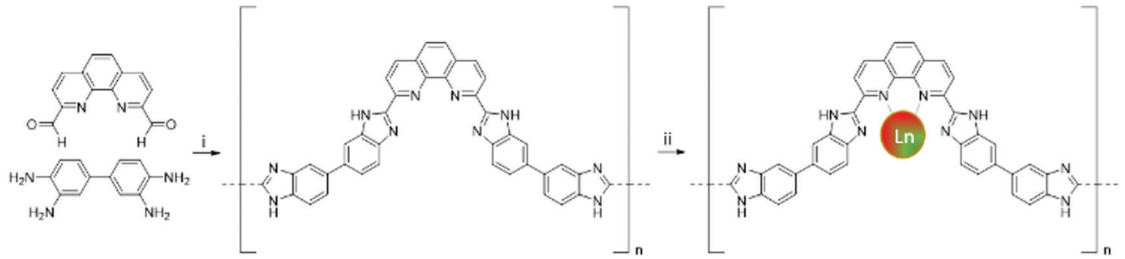

Fig. 1 Synthesis of the phen-polymer and grafting of the material with lanthanide complexes (Ln = Eu_tfac, Tb_tfac). Reaction conditions: (i) dioxane/mesitylene (3 : 2), 6 M HOAc, r.t., 48 h (ii). $Ln(tfac)_3{\cdot}2H_2O$, methanol, 80 °C, 24 h. The Ln^{3+} ions interact with the phen-polymer through coordination bonds.[25]

secondary amines at 3200 cm^{-1} and a peak at 1620 cm^{-1} for C=N stretching. The primary amines present in the starting material have clearly disappeared. The peak at 1705 cm^{-1} corresponds to the remaining aldehyde group at the termini of the polymer. The peak at 1603 cm^{-1} indicates C=N stretching in the phenanthroline ring. The peaks at 1585 cm^{-1} and 1500 cm^{-1} demonstrate stretching vibration of C=C bonds. The aromatic phenanthroline and biphenyl system shows peaks in the region of 858–700 cm^{-1} due to out-of-plane bending. The C–N stretching is indicated by peaks at 1350–1140 cm^{-1}.

The X-ray photoelectron spectroscopy N(1s) spectrum (Fig. 3A) represents two peaks, this indicates two bonding states of nitrogen atoms. The peak at 399.38 eV can be attributed to the amine (–NH–) group of the imidazole ring and the peak at 397.98–398.18 eV to the imine groups (C=N) of the imidazole and phenanthroline moieties. Thermogravimetric analysis was performed to investigate the temperature profile of the phen-polymer (Fig. 3B). The decomposition starts at around 400 °C and proceeds in a slow way. The phen-polymer is therefore stable in the investigated luminescent temperature range. The elemental analysis of the material reveals a relative nitrogen, carbon and hydrogen content of respectively 18.4%, 76.5% and 5.0%. The calculated experimental ratio of these values (N/C = 0.24) is in agreement with the theoretical obtained value (N/C = 0.25), taking into account aldehyde groups at the termini of the polymer. The PXRD pattern indicates that the phen-polymer is amorphous (Fig. SI3, ESI†) and BET surface area reveals a non-porous polymer (1 $m^2 g^{-1}$). MALDI-TOF analyses were also performed, but were inconclusive due to the complexity of the sample.

A successful grafting of Eu^{3+}–tfac complex is proven by TEM-EDX mapping images of nitrogen atoms and europium ions for

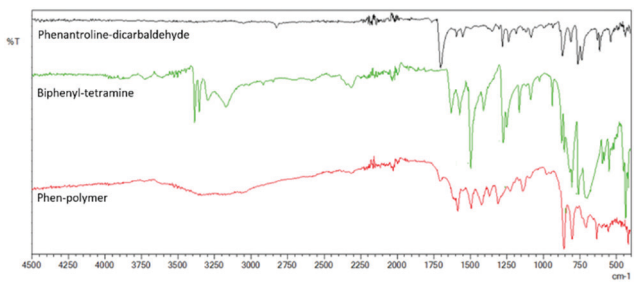

Fig. 2 FTIR spectra of the phen-polymer and the starting materials (1,10-phenanthroline-2,9-dicarbaldehyde and (1,1′-biphenyl)-3,3′,4,4′-tetramine).

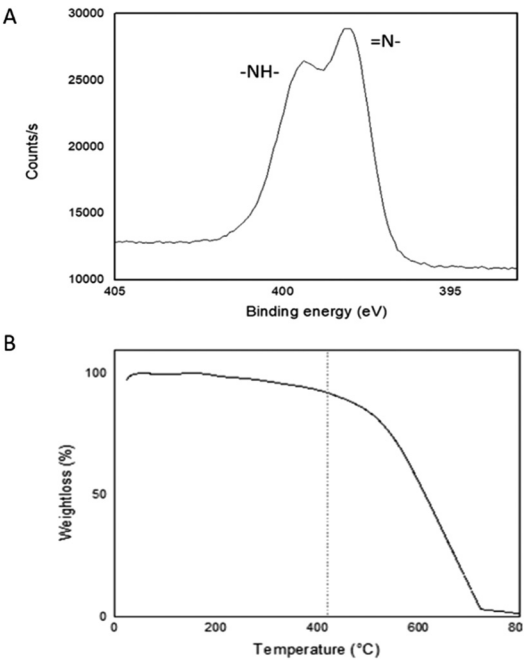

Fig. 3 Analysis of phen-polymer by (A) XPS N(1s) spectrum and (B) TG curve of the thermal degradation of the phen-polymer.

the phen-polymer@Eu_tfac (Fig. 4). The limited amount of dots outside the sample are a result of leakage due to ultrasonic-assisted sample preparation. Nitrogen atoms and Eu^{3+}–tfac complexes are uniformly distributed throughout the polymer. Thermogravimetric analysis of phen-polymer@Eu_tfac (Fig. SI4A, ESI†) shows a first decomposition of the sample at 200 °C and a second decomposition at 350 °C, indicating the presence of the metal complex and the phen-polymer. The grafted polymer is therefore stable in the investigated temperature region. A similar elemental distribution behavior and thermal curve is expected for the phen-polymer@Tb_tfac and phen-polymer@Eu,Tb_tfac. The phen-polymer@Eu,Tb_tfac is characterized by XPS and FTIR (Fig. SI4B, ESI†) to prove the successful coordination of Eu^{3+}- and Tb^{3+}–tfac complexes onto the polymer. The appearance of extra peaks in the FTIR spectra (Fig. SI4B, ESI†), compared to phen-polymer, in the region 1110–1290 cm^{-1} can be attributed to the presence of tfac. Furthermore, due to lanthanide coordination, a shift for C=N stretching can be seen at 1625 cm^{-1}. The oxidation states of the lanthanide ions in phen-polymer@Eu,Tb_tfac were

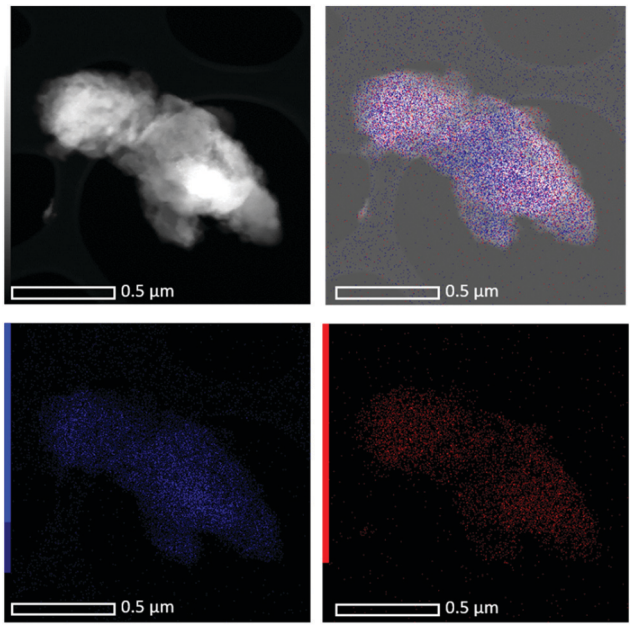

Fig. 4 HAADF-STEM and corresponding EDX mapping images of nitrogen (blue) and europium (red) for the sample of phen-polymer@Eu_tfac.

investigated through XPS analysis (Fig. 5). The characteristic peaks for Eu(III) $3d_{5/2}$ and Eu(III) $3d_{3/2}$ were observed at 1133.78 eV and 1163.68 eV, respectively.[31] During the measurement, a plausible reduction of Eu^{3+} to Eu^{2+} took place, resulting in peaks at 1124.58 eV and 1154.08 eV for Eu(II) $3d_{5/2}$ and Eu(II) $3d_{3/2}$. Furthermore, shake-up satellite peaks are also observed.[31] For Tb(III) $3d_{5/2}$ and Tb(III) $3d_{3/2}$ the characteristic peaks appeared at 1243.88 eV and 1278.18 eV, respectively. The difference between those peaks and their corresponding satellite peaks are 3.5 eV and 2.3 eV. Since this difference is smaller than 12 eV (the difference between Tb^{3+} and Tb^{4+}), the oxidation state of Tb is 3+.[32]

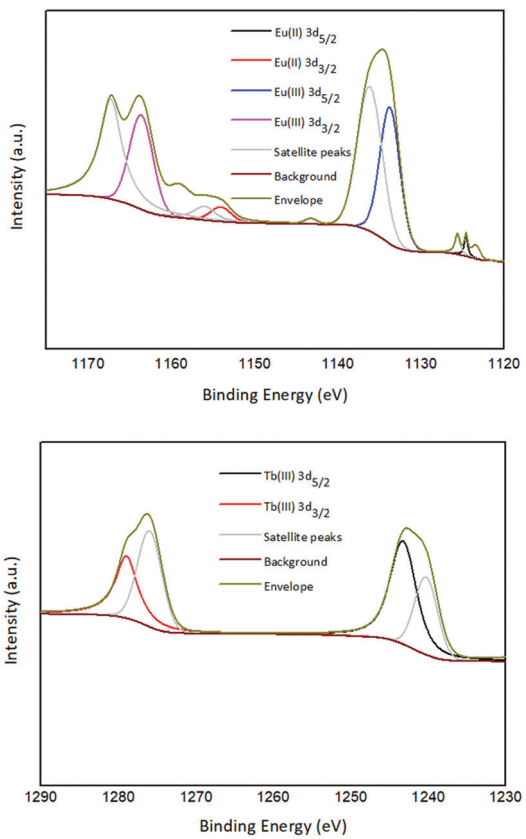

Fig. 5 Determination of oxidation state for Eu and Tb by XPS analysis for phen-polymer@Eu,Tb_tfac.

Luminescence study

The luminescence properties of the grafted phen-polymer were investigated. Fig. 6 shows a picture of the three prepared samples: phen-polymer@Eu_tfac, phen-polymer@Tb_tfac, and phen-polymer@Eu,Tb_tfac when placed under a UV lamp under 302 nm excitation. As can be seen under UV excitation, the emission colors are respectively red, green and yellow.

First, the room temperature excitation and emission spectra of the pristine (ungrafted) polymer sample were recorded. As can be seen in Fig. 7 the excitation spectrum consisted of a broad band from 250–425 nm, with a maximum at 372 nm. In the emission spectrum a broad band in the 400–550 nm range was observed, with a maximum at 438 nm.

The room temperature photoluminescence study of the phen-polymer@Eu_tfac material revealed a broad band in the

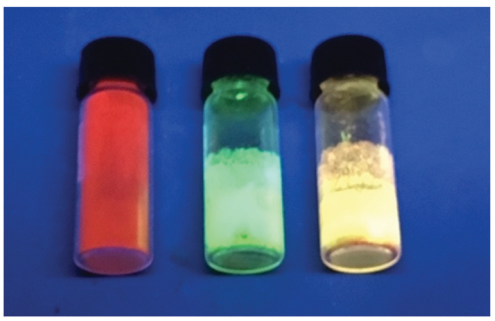

Fig. 6 Picture of samples (from left to right): phen-polymer@Eu_tfac, phen-polymer@Tb_tfac, and phen-polymer@Eu,Tb_tfac when placed under a UV lamp (at 302 nm excitation).

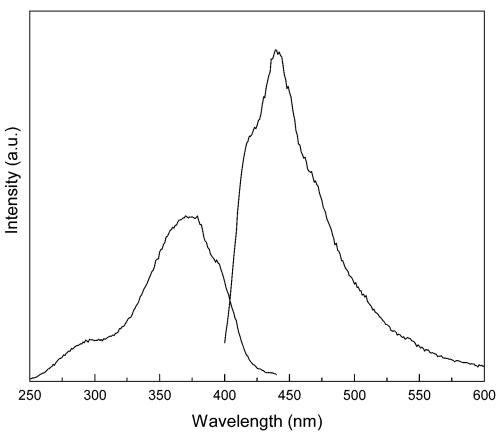

Fig. 7 Room temperature combined excitation–emission spectrum of phen-polymer (excited at 372 nm and observed at 438 nm).

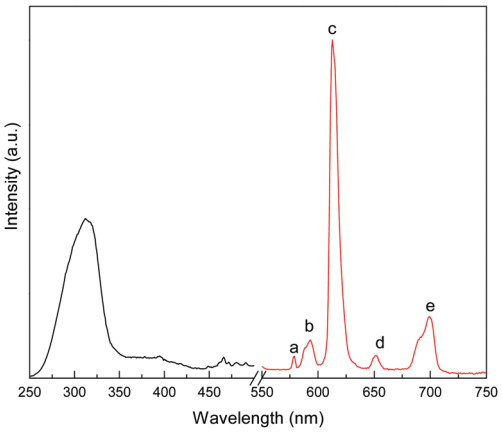

Fig. 8 Room temperature combined excitation–emission spectrum for phen-polymer@Eu_tfac material (excited at 312 nm, observed at 613 nm).

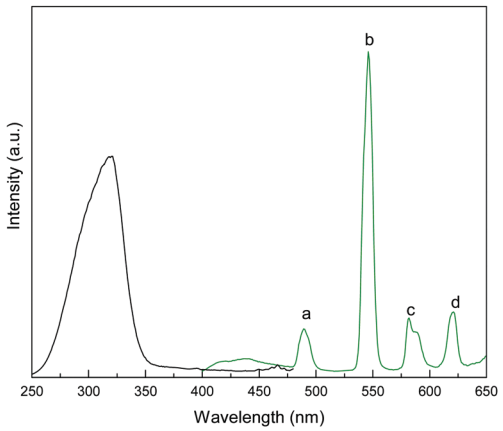

Fig. 9 Room temperature combined excitation–emission spectrum for phen-polymer@Tb_tfac material (excited at 319 nm, observed at 546 nm).

excitation spectrum around 250–350 nm, with a maximum at 312 nm (Fig. 8). After binding of the lanthanide a clear shift in the maximum of the broad band towards lower wavelengths is detected. A similar trend was observed for the other lanthanide grafted polymer samples. When exciting into the maximum of this band the characteristic transition peaks of Eu^{3+} are observed: $^5D_0 \rightarrow {}^7F_0$, $^5D_0 \rightarrow {}^7F_1$, $^5D_0 \rightarrow {}^7F_2$, $^5D_0 \rightarrow {}^7F_3$ and $^5D_0 \rightarrow {}^7F_4$. The transitions have been assigned to the appropriate peaks in Table 1. The luminescence decay time of the phen-polymer@Eu_tfac material was determined by fitting the curve with a biexponential function where t_1 = 306 μs and t_2 = 36 μs. The presence of two decay times indicated two different coordination environments of the Eu^{3+} ions grafted to the polymer. As one decay time (t_2) is significantly shorter, it must reside in an unfavorable environment (*e.g.* in the presence of several water molecules in its first coordination sphere).

Next, the room temperature photoluminescence study of the phen-polymer@Tb_tfac material revealed a broad band in the excitation spectrum around 250–350 nm, with a maximum at 319 nm (Fig. 9). When exciting into the maximum of this band the characteristic transition peaks of Tb^{3+} are observed: $^5D_4 \rightarrow {}^7F_6$, $^5D_4 \rightarrow {}^7F_5$, $^5D_4 \rightarrow {}^7F_4$, and $^5D_4 \rightarrow {}^7F_3$. The transitions have been assigned to the appropriate peaks in Table 2. The presence of a weak broad band in the emission spectrum in the 400–470 nm range suggests some incomplete energy transfer from the ligand to the Ln^{3+} ions. Furthermore, the decay time for this material was determined. The decay curve could only be well fitted employing a biexponential function, which yielded t_1 = 256 μs and t_2 = 47 μs. As in the Eu^{3+} material, the materials shows two decay times, which suggest two different coordination environments of the Tb^{3+} ions.

Table 1 Assignment of peaks labelled in Fig. 8

Peak	Wavelength (nm)	Wavenumber (cm^{-1})	Transition
		Emission	
a	578	17 301	$^5D_0 \rightarrow {}^7F_0$
b	592	16 892	$^5D_0 \rightarrow {}^7F_1$
c	613	16 313	$^5D_0 \rightarrow {}^7F_2$
d	650	15 384	$^5D_0 \rightarrow {}^7F_3$
e	699	14 306	$^5D_0 \rightarrow {}^7F_4$

Table 2 Assignment of peaks labelled in Fig. 9

Peak	Wavelength (nm)	Wavenumber (cm^{-1})	Transition
		Emission	
a	489	20 450	$^5D_4 \rightarrow {}^7F_6$
b	546	18 315	$^5D_4 \rightarrow {}^7F_5$
c	580	17 241	$^5D_4 \rightarrow {}^7F_4$
d	619	16 155	$^5D_4 \rightarrow {}^7F_3$

After determining the photoluminescence properties of the grafted phen-polymer with europium and terbium separately, a combined study was done. The room temperature combined excitation–emission spectrum of the phen-polymer@Eu,Tb_tfac (where Eu^{3+} and Tb^{3+} have been grafted at equal amounts) has been presented in Fig. 10. In the excitation spectrum, a broad band from 250–400 nm, with a maximum at 328 nm is observed. When exciting at 328 nm in the emission spectrum, we observe a range of both Tb^{3+} as well as Eu^{3+} emission peaks.

The peaks labeled a–g have been assigned to appropriate transitions in Table 3. At room temperature the intensity of the Eu^{3+} $^5D_0 \rightarrow {}^7F_2$ peak is slightly stronger than the Tb^{3+} $^5D_4 \rightarrow {}^7F_5$ peak. This results in a yellow emission color as shown in

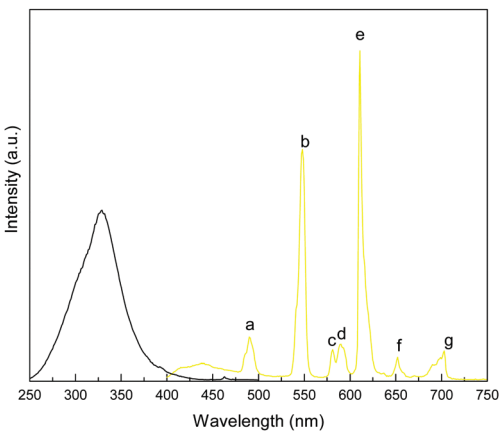

Fig. 10 Room temperature combined excitation–emission spectrum for phen-polymer@Eu,Tb_tfac material (excited at 328 nm, observed at 610 nm).

Table 3 Assignment of peaks labelled in Fig. 10

Peak	Wavelength (nm)	Wavenumber (cm^{-1})	Transition
		Emission	
a	490	20 408	$^5D_4 \rightarrow {}^7F_6$ (Tb)
b	548	18 248	$^5D_4 \rightarrow {}^7F_5$ (Tb)
c	579	17 271	$^5D_0 \rightarrow {}^7F_0$ (Eu)
d	591	16 920	$^5D_0 \rightarrow {}^7F_1$ (Eu)
e	610	16 393	$^5D_0 \rightarrow {}^7F_2$ (Eu)
f	653	15 314	$^5D_0 \rightarrow {}^7F_3$ (Eu)
g	703	14 224	$^5D_0 \rightarrow {}^7F_4$ (Eu)

Fig. 5. As in the phen-polymer@Tb_tfac material, the presence of a weak ligand band around 400–470 nm suggests some incomplete energy transfer from the ligand to the lanthanides.

The luminescence decay times of phen-polymer@Eu,Tb_tfac were also determined. For Eu^{3+} the decay curve could only be well fitted using a monoexponential decay curve, which yielded t = 1.03 ms. For Tb^{3+} the decay curve was fitted using a biexponential function yielding t_1 = 440 μs and t_2 = 138 μs. A huge increase in the Eu^{3+} decay time would suggest energy transfer from Tb^{3+} to Eu^{3+} in this polymer grafted with Eu^{3+}, Tb^{3+} tfac complexes. For all three lanthanide grafted phen-polymer compounds we determined the QY. It was calculated to be 4.7% for the phen-polymer@Eu_tfac, 7.1% for phen-polymer@Tb_tfac and 5.5% for phen-polymer@Eu,Tb_tfac.

We further investigated the temperature dependent luminescence properties of the phen-polymer@Eu,Tb_tfac material and considered its potential use as a luminescence ratiometric sensor. Thermometers based on the intensity (wavelength) ratio of two transitions (here, Eu^{3+} and Tb^{3+}) are called ratiometric thermometers and circumvent certain drawbacks such as fluctuations of the excitation source.[11] The emission spectra of the sample were recorded at varying temperatures, from 10–460 K. In the 10–260 K range the sample showed stable emission and could therefore not be used as a sensor in this temperature regime (Fig. 11A). In the 260–460 K range the sample showed monotonic behavior and was assessed for its use as a ratiometric thermometer (Fig. 11B).

The I_{548}/I_{610} ratio of the integrated areas was calculated (Tb^{3+}: 530–564; Eu^{3+}: 605–630). These data points could be well fitted employing the equation for Δ (R^2 = 0.99552) yielding Δ_0 = 2.5936, α = 99 924, ΔE = 2429 cm^{-1}. The nonradiative deactivation energies probably involve the $^5D_3$ level of Tb^{3+} (26 273 cm^{-1}) and the $^5D_3$ level of Eu^{3+} (24 408 cm^{-1}). The plot, showing the calibration curve, has been presented in Fig. 12. The maximum value of Sr was calculated to be 2.3404% K^{-1} (340 K) (Fig. 13), which indicates good thermometric behavior in this temperature regime. The emission color change of the material with temperature change has been indicated on the CIE color diagram in Fig. 14. The emission color of the compound changes from light green (260 K) to orange-red (460 K). Additionally, it is well known that materials consisting of Eu–Tb are excellent for usage in ratiometric temperature sensors as the two monitored peaks (here, at 548 nm and 610 nm) are well separated. This feature allows the materials to have a good signal discriminability for temperature detection.

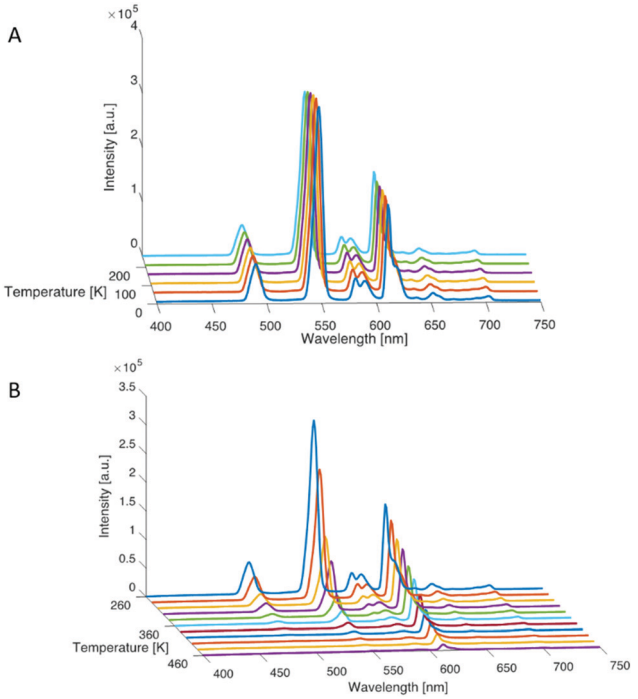

Fig. 11 Emission maps of the phen-polymer@Eu,Tb_tfac material recorded between (A). 10–260 K (step of 50 K) and (B). 260–460 K (step of 20 K).

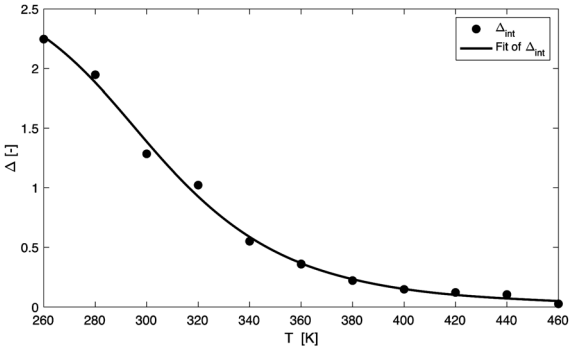

Fig. 12 Plot presenting the calibration curve for phen-polymer@Eu,Tb_tfac. The points show the experimental delta parameters. The solid line shows the best fit of the experimental points when the equation for Δ is employed.

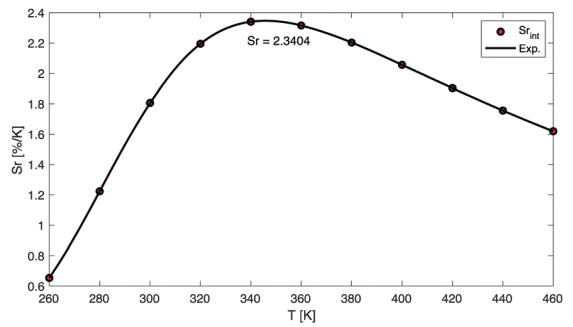

Fig. 13 Plot presenting the relative sensitivity Sr values at varied temperatures (260–460 K) for compound phen-polymer@Eu,Tb_tfac. The solid lines are guides for eyes.

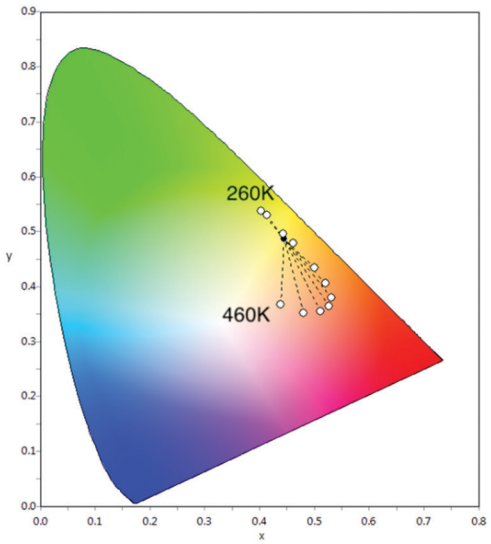

Fig. 14 CIE coordination diagram showing the x and y coordinates for phen-polymer@Eu,Tb_tfac recorded at different temperatures (260–460 K).

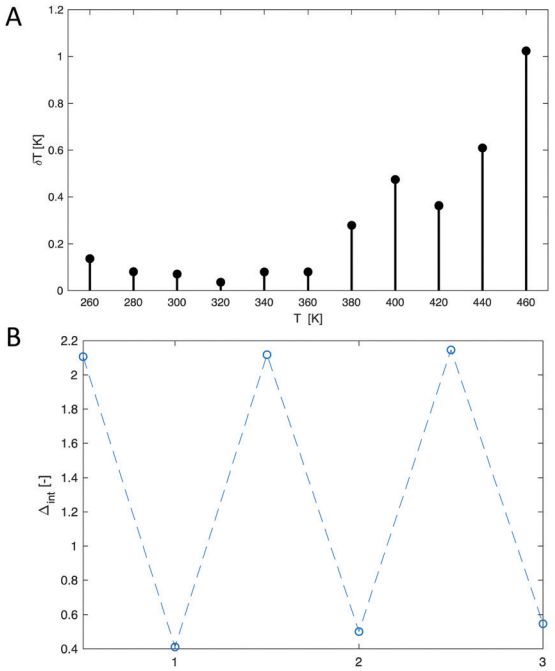

Fig. 15 (A) Calculated temperature uncertainty δT and (B) repeatability for phen-polymer@Eu,Tb_tfac.

The performance (maximum relative sensitivity, S_m) of the phen-polymer@Eu,Tb_tfac has been compared with the performances of other Eu–Tb materials previously reported in literature in Table 4. Our material shows a relative broad and defined temperature detection range, combined with a relative high maximum relative sensitivity. Additionally we have calculated the temperature uncertainty δT and we show that in almost the whole studied temperature range $\delta T < 1$ confirming its good behaviour as a temperature sensor (Fig. 15A). Repeatability tests were performed to analyse the behaviour of the material after heating and cooling. The repeatability was calculated to be up to 98% (Fig. 15B).

To better understand the energy transfer mechanism in the thermometer material the triplet level of the phen-polymer were determined at 77 K for a phen-polymer@Gd complex.

We have measured its photoluminescence in ethanol : methanol (4 : 1) solution at 77 K. In Fig. SI6A (ESI†) we have presented the RT emission spectrum and 77 K emission spectrum of the phen-polymer@Gd. To confirm that this is a triplet level band we have recorded the decay time at its maximum at 77 K and observed almost millisecond range lifetimes confirming the band belongs to a triplet level of the material (Fig. SI6B, ESI†). It is known that to determine the triplet level value one should take the high-energy edge of this band, which is around 415 nm (24 096 cm^{-1}). Therefore, with this measurement we confirm that the phen-polymer@Gd triplet level is more favorable for Tb^{3+} as it is located closer to the $^5D_4$ accepting level of Tb^{3+} than to the Eu^{3+} accepting levels. We can assume that upon UV excitation energy is transferred from the phen-polymer triplet level to the $^5D_4$ accepting level of Tb^{3+}, which is then further transferred (in part) to the $^5D_0$ accepting levels of Eu^{3+}. Emission of both Tb and Eu are observed.

Conclusions

We have developed an insoluble, purely organic phenanthroline-polymer, which can work as an antenna for Eu^{3+} and Tb^{3+} ions.

Table 4 Comparison of the relative intensity of other reported ratiometric lanthanide (Eu–Tb) based thermometers operating in a similar temperature regime. The materials, temperature range (K) and maximum relative sensitivity (S_m) have been overviewed

Material	Range (K)	S_m (% K^{-1})	Ref.
$[Tb(H_5btp)]\cdot H_2O$	299–319	1.66 (319 K)	33
$[Eu_2(qptca)(NO_3)_2(DMF)_4]\cdot(EtOH)_3 \subset$ perylene	293–353	1.28 (293 K)	34
$Tb_{0.8}Eu_{0.2}$BPDA	293–328	1.19 (313 K)	35
5 wt% Eu^{3+} doped alumina–phosphate glass	288–323	1.68 (288 K)	36
$Eu_{0.95}Tb_{0.05}$(BTC)	25–300	1.46 (300 K)	37
TbMOF@3%Eu_tfac	225–375	2.59 (225 K)	38
TbMOF@7.3%Eu_tfac	200–325	1.33 (325 K)	38
$Tb_{0.09}Eu_{0.01}(bdc)_{1.5}(H_2O)_2$	290–320	0.31 (318 K)	39
$Eu_{0.50}Tb_{0.50}$DPA·PMO	260–460	1.56 (360 K)	40
$Eu_{0.5}Tb_{0.5}(L)_1$@PMMA	77–297	0.46	21
$Eu_{0.05}Tb_{1.95}$-PDC	298–318	0.64 (318 K)	35
cycEu–phTb	10–200	1.86	22
Phen-polymer@Eu,Tb_tfac	260–460	2.34 (340 K)	This work

The incorporation of Eu^{3+}/Tb^{3+} in a 1:1 metal ratio yielded a material with both Eu^{3+} and Tb^{3+}, resulting in a yellow emission color. The clearly discriminable peaks of Eu^{3+} and Tb^{3+} allow the use of this system in ratiometric sensor applications. The temperature dependent luminescent properties of the novel insoluble phen-polymer were therefore investigated and the material was tested as ratiometric temperature sensor in the biological regime. The maximum value of the relative temperature sensitivity was calculated to be 2.3404% K^{-1} (340 K), which indicated good thermometric behavior. The emission color of the designed phen-polymer@Eu,Tb_tfac changed from light green (260 K) to orange-red (460 K).

Conflicts of interest

There are no conflicts to declare.

Acknowledgements

FVB thanks the Research Board of Ghent university (BOF GOA2017000303) for financial support. AMK thanks Ghent University for funding. The authors want to thank Katrien Haustraete for STEM/EDX mapping measurements, Prof. Rik Van Deun for access to the spectrophotometer, Prof. Karen Leus for her help with XPS and Eng. Pieter Naert for proofreading the manuscript.

References

1 P. R. N. Childs, J. R. Greenwood and C. A. Long, *Rev. Sci. Instrum.*, 2000, **71**, 2959–2978.
2 X. D. Wang, O. S. Wolfbeis and R. J. Meier, *Chem. Soc. Rev.*, 2013, **42**, 7834–7869.
3 T. Jüstel, J.-C. Krupa and D. U. Wiechert, *J. Lumin.*, 2001, **93**, 179.
4 A. A. Kaminskii, J. Garcia-Sole, J. Fernandez, R. Balda, H. J. Eichler, K.-I. Ueda, N. V. Klassen, B. S. Redkin, L. E. Li, J. Findeisen and D. Jaque, *Appl. Opt.*, 1999, **38**, 4533.
5 J.-C. Bunzli and C. Piguet, *Chem. Soc. Rev.*, 2005, **34**, 1048.
6 K. Binnemans, *Chem. Rev.*, 2009, **109**, 4283.
7 S. V. Eliseva and J.-C. Bunzli, *Chem. Soc. Rev.*, 2010, **39**, 189.
8 J. Rocha, C. D. S. Brites and L. D. Carlos, *Chem. – Eur. J.*, 2016, **22**, 14782.
9 Y. Cui, F. Zhu, B. Chen and G. Qian, *Chem. Commun.*, 2015, **51**, 7420.
10 Y. Hasegawa, Y. Miura, Y. Kitagawa, S. Wada, T. Nakanishi, K. Fushimi, T. Seki, H. Ito, T. Iwasa, T. Taketsuga, M. Gon, K. Tanaka, Y. Chujo, S. Hattori, M. Karasewa and K. Ishii, *Chem. Commun.*, 2018, **54**, 10695.
11 C. D. S. Brites, P. P. Lima, N. J. O. Silva, A. Millan, V. S. Amaral, F. Palacio and L. D. Carlos, *New J. Chem.*, 2011, **35**, 1177.
12 M. Ren, C. D. S. Brites, S. S. Bao, R. A. S. Ferreira, L. M. Zheng and L. D. Carlos, *J. Mater. Chem.*, 2015, **3**, 8480.
13 Y. Hasegawa, M. Yamamuro, Y. Wada, N. Kanehisa, Y. Kai and S. Yanagida, *J. Phys. Chem. A*, 2003, **107**, 1697.
14 R. Shunmugam and G. N. Tew, *J. Am. Chem. Soc.*, 2005, **127**(39), 13567–13572.
15 S. M. Borisov and I. J. Klimant, *Fluorescence*, 2008, **18**, 581–589.
16 X. Liu, S. Akerboom, M. de Jong, I. Mutikainen, S. Tanase, A. Meijerink and E. Bouwman, *Inorg. Chem.*, 2015, **54**, 11323.
17 A. Benayas, B. del Rosal, A. Perez-Delgado, K. Sanracruz-Gomez, D. Jaque, G. A. Hirata and F. Vetrone, *Adv. Opt. Mater.*, 2015, **3**, 687.
18 A. M. Kaczmarek, M. K. Kaczmarek and R. V. Deun, *Nanoscale*, 2019, **11**, 833.
19 A. M. Kaczmarek, J. Liu, B. Laforce, L. Vincze, K. Van Hecke and R. V. Deun, *Dalton Trans.*, 2017, **46**, 5781.
20 A. M. Kaczmarek, *J. Mater. Chem. C*, 2018, **6**, 5916.
21 H. Li, S. Wang, C. Tian, D. Liu and D. Yang, *J. Colloid Interface Sci.*, 2018, **519**, 11–17.
22 G. Bao, K. Wong, D. Jin and P. A. Tanner, *Light: Sci. Appl.*, 2018, **7**, 96.
23 X. Wu, D. Zhang, Y. Liang, K. Zhang, Q. Liu, L. Dong and C. Shan, *Dalton Trans.*, 2019, **48**, 7910–7917.
24 D. Mara, F. Artizzu, B. Laforce, L. Vincze, K. Van Hecke, R. Van Deun and A. M. Kaczmarek, *J. Lumin.*, 2019, **213**, 343–355.
25 J.-C. Bunzli and C. Piguet, *Chem. Rev.*, 2002, **102**(6), 1897–1928.
26 R. Geitenbeek, B. B. V. Salzmann, A.-E. Nieuwelink, A. Meijerink and B. M. Weckhuysen, *Chem. Eng. Sci.*, 2019, **198**, 235–240.
27 R. Geitenbeek, A.-E. Nieuwelink, T. S. Jacobs, B. B. V. Salzmann, J. Goetze, A. Meijerink and B. M. Weckhuysen, *ACS Catal.*, 2018, **8**(3), 2397–2401.
28 J. Yu, L. Sun, H. Peng and M. I. J. Stich, *J. Mater. Chem.*, 2010, **20**, 6975–6981.
29 N. T. Coogan, M. A. Chimes, J. Raftery, P. Mocilac and M. A. Denecke, *J. Org. Chem.*, 2015, **80**, 8684–8693.
30 O. Valdes, C. E. Vergara, M. B. Camarada, V. Carrasco-Sanchez, F. M. Nachtigall, J. Tapia, R. Fischer, F. D. Gonzalez-Nilo and L. S. Santos, *J. Environ. Manage.*, 2015, **147**, 321–329.
31 F. Mercier, C. Alliot, L. Bion, N. Thromat and P. Toulhoat, *J. Electron Spectrosc. Relat. Phenom.*, 2006, **150**, 21–26.
32 G. Kalkowski, G. Kaindl and G. Wortmann, *Phys. Rev. B: Condens. Matter Mater. Phys.*, 1988, **37**, 1376–1382.
33 D. Ananias, A. D. G. Firmino, R. F. Mendes, F. A. Almeida Paz, M. Nolasco, L. D. Carlos and J. Rocha, *Chem. Mater.*, 2017, **29**, 9547.
34 Y. Cui, R. Song, J. Yu, M. Liu, Z. Wang, C. Wu, Y. Yang, Z. Wang, B. Chen and G. Qian, *Adv. Mater.*, 2015, **27**, 1420.
35 D. Zhao, X. Rao, J. Yu, Y. Cui, Y. Yang and G. Qian, *Inorg. Chem.*, 2015, **54**, 11193.
36 C. Y. Morassuti, L. A. O. Nunes, S. M. Lima and L. H. C. Andrade, *J. Lumin.*, 2018, **193**, 39.
37 X. Zhou, L. Chen, Z. Feng, S. Jiang, J. Lin, Y. Pang, L. Li and G. Xiang, *Inorg. Chim. Acta*, 2018, **469**, 576.
38 A. M. Kaczmarek, Y.-Y. Liu, C. Wang, B. Laforce, L. Vincze, P. Van Der Voort and R. V. Deun, *Dalton Trans.*, 2017, **46**, 12717.
39 A. Cadiau, C. D. S. Brites, P. M. F. J. Costa, R. A. S. Ferreira, J. Rocha and L. D. Carlos, *ACS Nano*, 2013, **7**, 7213.
40 A. M. Kaczmarek, R. Van Deun and P. Van Der Voort, *J. Mater. Chem. C*, 2019, **7**, 4222.

